MMSE based QRM-MLD Frequency-domain Block Signal Detection for Single-carrier Transmission

Tetsuya YAMAMOTO† Kazuki TAKEDA† and Fumiyuki ADACHI‡
Dept. of Electrical and Communication Engineering, Graduate School of Engineering, Tohoku University
6-6-05 Aza-Aoba, Aramaki, Aoba-ku, Sendai, 980-8579 Japan
†{yamamoto, kazuki}@mobile.ecei.tohoku.ac.jp, ‡adachi@ecei.tohoku.ac.jp

***Abstract*—In this paper, we propose an improved frequency-domain block signal detection (FDBD) using minimum mean square error (MMSE) based maximum likelihood detection (MLD) employing QR decomposition and M-algorithm (QRM-MLD) for the single-carrier (SC) block transmissions. In the conventional FDBD with QRM-MLD, if the number of surviving symbol candidates is small, the achievable bit error rate (BER) performance degrades, because the probability of removing the correct symbol candidates at early stages increases. In this paper, to solve this problem, we propose an FDBD using MMSE QRM-MLD and show by computer simulation that the MMSE QRM-MLD can reduce the number of surviving symbol-candidates to 1/4 of the conventional QRM-MLD in order to achieve the bit error rate (BER) performance close to the matched filter bound and can reduce the overall complexity to 30% when 16QAM is used.**

Keywords-component; Single-carrier, QRM-MLD, frequency-domain signal detection

I. INTRODUCTION

In next generation mobile communication systems, broadband data services are demanded. Since the mobile wireless channel is composed of many propagation paths with different time delays, the channel becomes severely frequency-selective as the transmission data rate increases. When single-carrier (SC) transmission without equalization technique is used, the bit error rate (BER) performance significantly degrades due to inter-symbol interference (ISI) [1]. A cyclic prefixed SC (CP-SC) block transmission with simple one-tap frequency-domain equalization (FDE) based on the minimum mean square error criterion (MMSE) can significantly improve the BER performance in a frequency-selective fading channel [2, 3]. However, due to the presence of residual ISI after FDE, a big performance gap still exists from the matched filter (MF) bound [4]. To narrow the performance gap, a frequency-domain iterative ISI cancellation technique combined with MMSE-FDE was proposed in [4, 5]. However, the achievable BER performance is still a few dB away from the MF bound.

Recently, we proposed a frequency-domain block signal detection (FDBD) using maximum likelihood detection (MLD) employing QR decomposition and M-algorithm (QRM-MLD) [6] for the SC block transmissions. We showed that the FDBD using QRM-MLD significantly improves the BER performance compared to the MMSE-FDE and achieves BER performance close to the MF bound by increasing the number of surviving symbol-candidates. In FDBD using QRM-MLD, the concatenation of the fast Fourier transform (FFT) and the propagation channel is regarded as an equivalent channel, to which the QR decomposition is applied. The received signal power depends on the elements of an upper triangular matrix **R**, obtained by QR-decomposition of the equivalent channel matrix. However, in the case of SC transmission, the amplitude of an element of **R** closer to lower right positions may drop [7]. If the number of surviving symbol-candidates is small, the achievable BER performance degrades because the probability of removing the correct symbol-candidates at early stages increases. If this probability can be reduced, the achievable BER performance of QRM-MLD can be improved. One solution is to increase the number of surviving symbol-candidates. However, this increases the computational complexity.

In this paper, to mitigate the amplitude drop of the elements of **R** and hence to avoid the increase in the computational complexity, we propose an FDBD using MMSE QRM-MLD for the SC block transmissions. The MMSE QRM-MLD was originally proposed for MIMO signal transmissions [8, 9]. It was shown [8, 9] that the number of surviving symbol-candidates can be reduced to half of the original QRM-MLD in order to achieve the same performance for 4×4 MIMO systems. In this paper, we show by computer simulation that the FDBD using MMSE QRM-MLD can achieve close to the MF bound while reducing the number of surviving symbol-candidates.

The remainder of this paper is organized as follows. Sect. II presents the principle of FDBD using MMSE QRM-MLD. In Sect. III, we discuss the computer simulation results. Sect. IV offers the conclusion.

II. FDBD USING MMSE QRM-MLD

A. Transmission System

The SC transmission system model is illustrated in Fig. 1. Throughout the paper, the symbol-spaced discrete time representation is used. At the transmitter, a binary information sequence is data-modulated and then, the data-modulated symbol sequence is divided into a sequence of signal blocks of N_c symbols each, where N_c is the size of fast Fourier transform (FFT). The data symbol block is expressed using the vector form as $\mathbf{d}=[d(0),\ldots d(n),\ldots,d(N_c-1)]^T$. The last N_g symbols of

each block are copied as a CP and inserted into the guard interval (GI) placed at the beginning of each block and a CP-inserted data block of N_c+N_g symbols is transmitted.

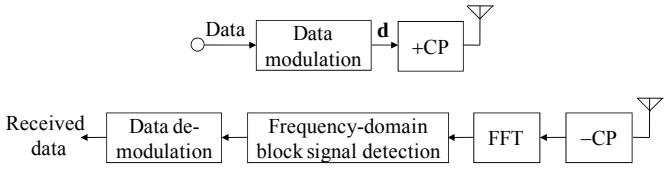

(a) SC transmission system model.

Figure 1. SC block transmission.

B. Received Signal

We assume a symbol-spaced frequency-selective fading channel composed of L distinct propagation paths. The channel impulse response $h(\tau)$ is given by

$$h(\tau)=\sum_{l=0}^{L-1}h_l\delta(\tau-\tau_l)\,, \tag{1}$$

where h_l and τ_l are respectively the complex-valued path gain with $E[\sum_{l=0}^{L-1}|h_l|^2]=1$ and the time delay of the lth path. The CP-removed received signal block $\mathbf{y}=[y(0),...,y(t),...,y(N_c-1)]^T$ can be expressed using the vector form as

$$\mathbf{y}=\sqrt{2E_s/T_s}\mathbf{hd}+\mathbf{n}\,, \tag{2}$$

where E_s and T_s are respectively the symbol energy and the symbol duration, $\mathbf{h}$ is the $N_c\times N_c$ channel impulse response matrix given as

$$\mathbf{h}=\begin{bmatrix} h_0 & & & & h_{L-1} & & h_1 \\ h_1 & h_0 & & & & \ddots & \vdots \\ \vdots & h_1 & h_0 & \mathbf{0} & & & h_{L-1} \\ h_{L-1} & \vdots & h_1 & \ddots & & & \\ & h_{L-1} & \vdots & & h_0 & & \\ & & h_{L-1} & & h_1 & \ddots & \\ \mathbf{0} & & & \ddots & \vdots & & h_0 \end{bmatrix}, \tag{3}$$

and $\mathbf{n}=[n(0),...,n(t),...,n(N_c-1)]^T$ is the noise vector. The tth element, $n(t)$, of $\mathbf{n}$ is the zero-mean additive white Gaussian noise (AWGN) having the variance $2N_0/T_s$ with N_0 being the one-sided noise power spectrum density.

C. Frequency-domain Received Signal

N_c-point FFT is applied to transform the received signal block into the frequency-domain signal vector $\mathbf{Y}=[Y(0),\ldots,Y(k),...,Y(N_c-1)]^T$. $\mathbf{Y}$ is expressed as

$$\mathbf{Y}=\mathbf{Fy}=\sqrt{2E_s/T_s}\mathbf{Fhd}+\mathbf{Fn}\,, \tag{4}$$

where $\mathbf{F}$ is the FFT matrix of size $N_c\times N_c$ given by

$$\mathbf{F}=\frac{1}{\sqrt{N_c}}\begin{bmatrix} 1 & 1 & \cdots & 1 \\ 1 & e^{-j2\pi\frac{1\times 1}{N_c}} & \cdots & e^{-j2\pi\frac{1\times(N_c-1)}{N_c}} \\ \vdots & \vdots & \ddots & \vdots \\ 1 & e^{-j2\pi\frac{(N_c-1)\times 1}{N_c}} & \cdots & e^{-j2\pi\frac{(N_c-1)\times(N_c-1)}{N_c}} \end{bmatrix}. \tag{5}$$

Due to the circulant property of $\mathbf{h}$ [10], we have

$$\mathbf{FhF}^H=diag[H(0),\ldots,H(k),...,H(N_c-1)]\equiv\mathbf{H}\,, \tag{6}$$

where $H(k)=\sum_{l=0}^{L-1}h_l\exp(-j2\pi k\tau_l/N_c)$, k=0~N_c–1, and $(.)^H$ is the Hermitian transpose operation. Using Eq. (6), Eq. (4) can be rewritten as

$$\mathbf{Y}=\sqrt{2E_s/T_s}\mathbf{HFd}+\mathbf{N}=\sqrt{2E_s/T_s}\overline{\mathbf{H}}\mathbf{d}+\mathbf{N}\,, \tag{7}$$

where $\overline{\mathbf{H}}=\mathbf{HF}$ and $\mathbf{N}=[N(0),...,N(k),...,N(N_c-1)]^T$ are respectively the equivalent channel matrix and the frequency-domain noise vector.

D. Conventional QRM-MLD

In the case of SC transmissions, all symbols have the same signal-to-interference plus noise power ratio (SINR) and hence, no ordering is necessary. First, applying the QR decomposition to the equivalent channel matrix $\overline{\mathbf{H}}$, we have $\overline{\mathbf{H}}=\mathbf{QR}$, where $\mathbf{Q}$ is an $N_c\times N_c$ matrix satisfying $\mathbf{Q}^H\mathbf{Q}=\mathbf{I}$ and $\mathbf{R}$ is an $N_c\times N_c$ upper triangular matrix. The transformed frequency-domain received signal $\hat{\mathbf{Y}}$ is obtained as

$$\begin{aligned}\hat{\mathbf{Y}}&=\mathbf{Q}^H\mathbf{Y}=\sqrt{2E_s/T_s}\mathbf{Rd}+\mathbf{Q}^H\mathbf{N}\\&=\sqrt{\frac{2E_s}{T_s}}\begin{bmatrix} R_{0,0} & R_{0,1} & \cdots & R_{0,N_c-1} \\ & R_{1,1} & \cdots & R_{1,N_c-1} \\ & & \ddots & \vdots \\ \mathbf{0} & & & R_{N_c-1,N_c-1} \end{bmatrix}\begin{bmatrix} d(0) \\ d(1) \\ \vdots \\ d(N_c-1) \end{bmatrix}.\\&\quad+\mathbf{Q}^H\mathbf{N}\end{aligned} \tag{8}$$

The M-algorithm [11] is composed of N_c stages, each stage being used to detect one of N_c symbol in a block. In the nth (0~N_c–1) stage, the path metric based on the squared Euclidean distance is computed using the nth element of $\hat{\mathbf{Y}}$, the nth row of $\mathbf{R}$, and the surviving symbol-candidates associated with symbols $d(N_c-1)$~$d(N_c-1-n)$. Then, the accumulated metric, which is the sum of the path metric and the accumulated metric at the previous stage, is computed. The best M symbol-candidates are selected by comparing the accumulated metrics associated with all surviving symbol-candidates at the present stage and are passed to the next stage.

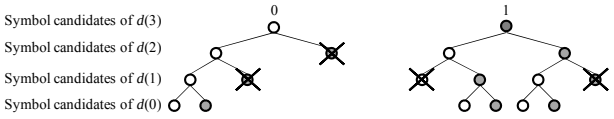

Figure 2. An example of QRM-MLD (M=3) with BPSK when N_c=4.

An example of the QRM-MLD is shown in Fig. 2 assuming N_c=4, binary phase shift keying (BPSK) modulation, and M=3. In the first stage, the accumulated metric based on the squared Euclidean distance between $\hat{Y}(N_c-1)$ and each symbol-candidate is computed using

$$e_0 = \left|\hat{Y}(N_c-1) - \sqrt{2E_s/T_s}R_{N_c-1,N_c-1}\bar{d}(N_c-1)\right|^2. \quad (9)$$

In Eq. (9), $\bar{d}(N_c-1)$ is the symbol-candidate for $d(N_c-1)$. Then, $\min\{M, X\}$ symbol-candidates having the smallest accumulated metric are selected as surviving symbol-candidate for $d(N_c-1)$, where X denotes the modulation level of QAM. The surviving symbol-candidates are transferred to the next stage. In the second stage, there are a total of X symbol-candidates for $d(N_c-2)$ leaving from each of surviving symbol-candidate for $d(N_c-1)$ selected at the previous stage. Therefore, there are a total of $M\cdot X$ possible combinations of $d(N_c-1)$ and $d(N_c-2)$. The accumulated metrics are computed for all possible $M\cdot X$ combinations using

$$e_1 = \sum_{n=0}^{1}\left|\hat{Y}(N_c-1-n) - \sqrt{\frac{2E_s}{T_s}}\sum_{i=0}^{n}R_{N_c-1-n,N_c-1-i}\bar{d}(N_c-1-i)\right|^2. \quad (10)$$

Similar to the first stage, M surviving symbol-candidates are selected from $M\cdot X$ combinations of $d(N_c-1)$ and $d(N_c-2)$. This procedure is repeated until the last stage (n=N_c–1). The accumulated metric at the nth stage is calculated using

$$e_n = \sum_{n'=0}^{n}\left|\hat{Y}(N_c-1-n') - \sqrt{\frac{2E_s}{T_s}}\sum_{i=0}^{n'}R_{N_c-1-n',N_c-1-i}\bar{d}(N_c-1-i)\right|^2. \quad (11)$$

The most possible transmitted symbol sequence is found by tracing back the path starting from the symbol-candidate having the smallest accumulated metric at the last stage (n=N_c–1). QRM-MLD requires $X\{1+M(N_c-1)\}$ times squared Euclidean distance calculation, which is significantly smaller than the original MLD which requires X^{N_c} times squared Euclidean distance calculation.

However, the use of a large M is necessary in order to achieve the performance close to the full MLD. For example, for 16QAM modulation, M=256 is necessary when N_c=64 [6].

E. MMSE QRM-MLD

The received signal power associated with the symbol $d(N_c-1-i)$ at the nth stage ($n\geq i$, n=0~N_c–1) is the sum of the squared values of the (N_c–1–i)~(N_c–1)th elements in the (N_c–1–i)th column of $\mathbf{R}$. Therefore, the probability of removing the correct symbol-candidates is greater at an earlier stage since the received signal power is smaller at an earlier stage. Furthermore, in the case of SC transmission, since the channel impulse response matrix is represented by a circulant matrix, the amplitude of the element of $\mathbf{R}$ closer to lower right position drops [7]. This indicates that when small M is used, the probability of removing the correct symbol-candidates at an earlier stage increases. The selection error at an earlier stage greatly affects the achievable BER performance since the MLD based on the M-algorithm successively reduces the symbol candidate stage-by-stage. Therefore, to improve the BER performance, this probability must be reduced. If large M is used, this probability can be reduced, but at the cost of increased computational complexity.

To reduce the number of surviving symbol-candidates, we apply the MMSE QRM-MLD, which was originally proposed for MIMO transmission systems [8, 9], to the SC FDBD. In the MMSE QRM-MLD, the drop in the amplitude the element of $\mathbf{R}$ closer to lower right positions can be prevented by using the MMSE based QR decomposition [8]. As a result, it can be expected that the probability of removing the correct symbol-candidates at an earlier stage will be reduced even if small M is used. Therefore, the number of surviving symbol-candidates can be reduced in order to achieve the same BER performance as the conventional QRM-MLD.

In the MMSE QRM-MLD [9], first, we introduce a $2N_c\times N_c$ extended equivalent channel matrix $\overline{\mathbf{H}}^{ext}$ and a $2N_c\times 1$ extended frequency-domain received signal vector $\mathbf{Y}^{ext}$:

$$\overline{\mathbf{H}}^{ext} = \begin{bmatrix}\overline{\mathbf{H}} \\ \sqrt{N_0/E_s}\mathbf{I}_{N_c}\end{bmatrix}, \quad \mathbf{Y}^{ext} = \begin{bmatrix}\mathbf{Y} \\ \mathbf{0}_{N_c\times 1}\end{bmatrix}, \quad (12)$$

where $\mathbf{I}_{N_c}$ is an $N_c\times N_c$ identity matrix and $\mathbf{0}_{N_c\times 1}$ is a zero column vector of length N_c. Next, applying the QR decomposition to the extended equivalent channel matrix $\overline{\mathbf{H}}^{ext}$, we have $\overline{\mathbf{H}}^{ext} = \widetilde{\mathbf{Q}}\widetilde{\mathbf{R}}$, where $\widetilde{\mathbf{Q}}$ is a $2N_c\times N_c$ matrix satisfying $\widetilde{\mathbf{Q}}^H\widetilde{\mathbf{Q}} = \mathbf{I}$ and $\widetilde{\mathbf{R}}$ is an $N_c\times N_c$ upper triangular matrix. The transformed frequency-domain received signal $\widetilde{\mathbf{Y}}$ is obtained as

$$\widetilde{\mathbf{Y}} = \widetilde{\mathbf{Q}}^H\mathbf{Y}^{ext} = \sqrt{\frac{2E_s}{T_s}}\widetilde{\mathbf{R}}\mathbf{d} + \widetilde{\mathbf{Q}}^H\begin{bmatrix}\mathbf{N} \\ -\sqrt{N_0/E_s}\mathbf{d}\end{bmatrix}. \quad (13)$$

From Eq. (13), the ML solution is obtained by carrying out,

$$\hat{\mathbf{d}} = \arg\min_{\bar{\mathbf{d}}\in X^{N_c}}\left\{\left\|\widetilde{\mathbf{Y}} - \sqrt{\frac{2E_s}{T_s}}\widetilde{\mathbf{R}}\bar{\mathbf{d}}\right\|^2 - \frac{N_0}{E_s}\left\|\bar{\mathbf{d}}\right\|^2\right\}. \quad (14)$$

where $\bar{\mathbf{d}}$ is a symbol-candidate vector. In MMSE QRM-MLD, M-algorithm is applied to Eq. (14), in the same way as in the conventional QRM-MLD, the MLD based on the M-algorithm can be done using $\widetilde{\mathbf{Y}}$, $\widetilde{\mathbf{R}}$, and symbol-candidates.

III. COMPUTER SIMULATION

The condition for the computer simulation is shown in Table 1. We assume the FFT block size of N_c=64 symbols and the length of CP is N_g=16 symbols. The channel is assumed to be a symbol-spaced L=16-path frequency-selective block Rayleigh fading channel having uniform power delay profile. Ideal channel estimation is assumed.

TABLE I. COMPUTER SIMULATION CONDITION

Transmitter	Modulation	QPSK, 16QAM
	Size of FFT	N_c=64
	Length of CP	N_g=16
Channel	Fading type	Frequency-selective block Rayleigh
	Power delay profile	L=16-path uniform power delay profile
	Time delay	$\tau_l=l$ (l=0~L−1)
Receiver	Channel estimation	Ideal

The average BER performance achievable with the MMSE QRM-MLD is plotted in Fig. 3 as a function of average received bit energy-to-noise power spectrum density ratio E_b/N_0(=$(E_s/N_0)(1+N_g/N_c)/\log_2 X$). Three cases of the number M of surviving symbol-candidates in each stage are plotted (i.e., M=1, 4, and 16 for QPSK and M=1, 16, and 64 for 16QAM). For comparison, the performance achievable with the conventional QRM-MLD is plotted. Also plotted is the MF bound [12]. When small M is used, the achievable BER performance with the conventional QRM-MLD degrades because the probability of removing the correct symbol-candidates at early stages increases. On the other hand, the MMSE QRM-MLD can achieve better BER even if small M is used. The reason for this is discussed below.

Figure 4 shows the probability density function (pdf) of the squared value of R_{N_c-1,N_c-1} (the received signal power associated with the symbol to be detected at the first stage) when E_b/N_0=10dB (16QAM). It is seen that when the QRM-MLD is used, the probability that the received signal power drops is high and therefore, the probability of removing the correct symbol-candidates at first stages increases when small M is used. On the other hand, the MMSE QRM-MLD can reduce the probability that the received signal power drops and therefore, the probability of removing the correct symbol-candidates at earlier stages can be reduced.

Figure 5 plots the required E_b/N_0 of the QRM-MLD or the MMSE QRM-MLD for achieving BER=10^{-3} as a function of M. For comparison, the required E_b/N_0 for MF is also plotted. When the QRM-MLD is used, M=64(256) is necessary to achieve the BER performance close to the MF bound for QPSK (16QAM). However, when the MMSE QRM-MLD is used, the achievable BER performance approaches the MF bound if M=16(64) is used for QPSK (16QAM). The performance gap of 0.97dB from the MF bound is owing to the loss due to the insertion of CP.

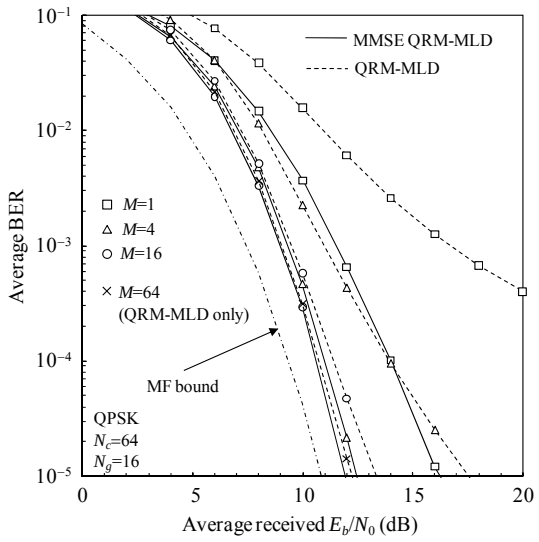

(a) QPSK(X=4)

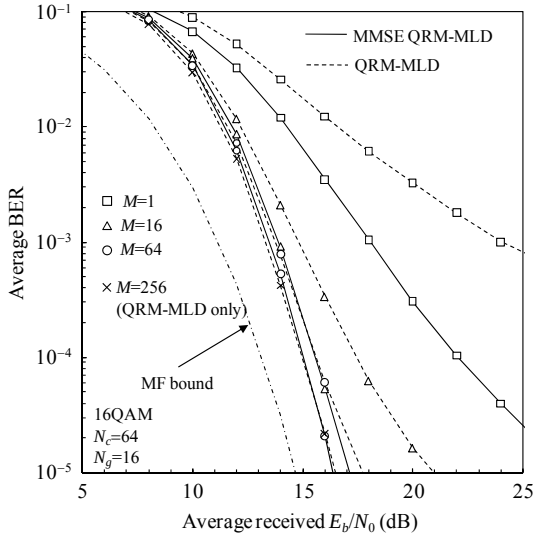

(b) 16QAM(X=16)

Figure 3. Average BER performance.

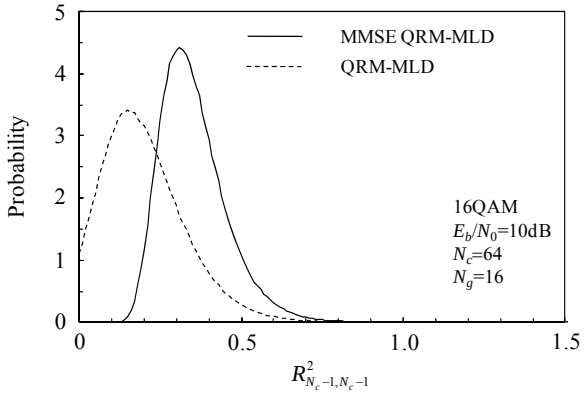

Figure 4. PDF of $R^2_{N_c-1,N_c-1}$.

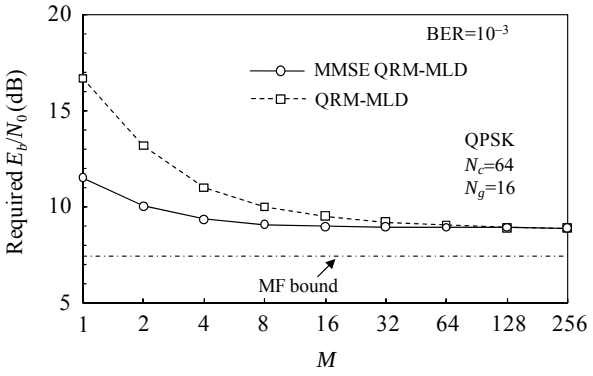

(a) QPSK(X=4)

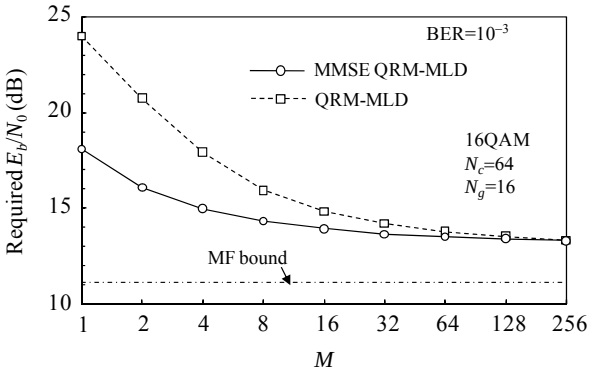

(b) 16QAM(X=16)

Figure 5. Required average received E_b/N_0 as a function of the number M of surviving symbol-candidates.

The computational complexity, defined as the number of complex multiplications, of the FDBD using MMSE QRM-MLD is compared with that of the FDBD using the conventional QRM-MLD. The number of multiplications is given in Table 2. For both QRM-MLD and MMSE-QRM-MLD, the number of multiplications is $N_c \times \log_2 N_c$ for FFT, N_c^2 for the transformation of the frequency-domain received signal after QR decomposition, and $X\{2+(M/2)(N_c+4)(N_c-1)\}$ for the squared Euclidean distance calculation. The number of multiplications for the QR decomposition is $2N_c^3$ in the case of MMSE QRM-MLD, which is two times that of the conventional QRM-MLD. However, as mentioned earlier, the MMSE QRM-MLD can reduce the number of surviving symbol-candidates to 1/4 of the conventional QRM-MLD (from M=64 to M=16 for QPSK and from M=256 to M=64 for 16QAM). As a result, the computational complexity of MMSE QRM-MLD is about 82(30) % of the conventional QRM-MLD when QPSK (16QAM) is used. Although FDBD using MMSE QRM-MLD achieves BER performance close to the MF bound while reducing the computational complexity compared to the conventional QRM-MLD, its complexity is still higher than that of MMSE-FDE (about 4800 times when 16QAM is used). Therefore, a further complexity reduction is necessary and it is left as an important future study.

TABLE II. NUMBER OF MULTIPLICATIONS

	MMSE QRM-MLD	QRM-MLD
FFT	$N_c \times \log_2 N_c$	$N_c \times \log_2 N_c$
QR decomposition	$2N_c^3$	N_c^3
Multiplication of $\mathbf{Q}^H$	N_c^2	N_c^2
Squared Euclidian distance calculations	$X\{2+(M/2)(N_c+4)(N_c-1)\}$	$X\{2+(M/2)(N_c+4)(N_c-1)\}$

IV. CONCLUSIONS

In this paper, we proposed the FDBD using MMSE QRM-MLD to improve the BER performance of SC transmissions. We showed by computer simulation that the MMSE QRM-MLD can achieve close to the MF bound while reducing the number of surviving symbol-candidates (and thus, reducing the overall computational complexity) compared to the conventional QRM-MLD. When QPSK (16QAM) is used, the MMSE QRM-MLD can reduce the number of surviving symbol-candidates to 1/4 of the conventional QRM-MLD and hence reduce the overall complexity to 82(30)% of the conventional QRM-MLD.

REFERENCES

[1] J. G. Proakis and M. Salehi, *Digital communications*, 5th ed., McGraw-Hill, 2008.

[2] D. Falconer, S. L. Ariyavisitakul, A. Benyamin- Seeyar B. Edison, "Frequency domain equalization for single-carrier broadband wireless systems," IEEE Commun. Mag., Vol. 40, No. 4, pp. 58-66. Apr. 2002.

[3] K. Takeda, T. Itagaki, and F. Adachi, "Joint use of frequency-domain equalization and transmit/receive antenna diversity for single-carrier transmissions," IEICE Trans. Commun., vol. E87-B, No. 7, pp.1946-1953, Jul. 2004.

[4] N. Benvenuto and S. Tomasin, "Block iterative DFE for single carrier modulation," Electron. Lett., Vol. 38, No. 19, pp. 1144-1145, Sep. 2002.

[5] K. Takeda, K. Ishihara and F. Adachi, "Frequency-domain ICI cancellation with MMSE equalization for DS-CDMA downlink," IEICE Trans. Commun., Vol. E89-B, No. 12, pp. 3335-3343, Dec. 2006.

[6] T. Yamamoto, K. Takeda, and F. Adachi, "Single-carrier transmission using QRM-MLD with antenna diversity," The 12th International Symposium on Wireless Personal Multimedia Communications (WPMC 2009), Sendai, Japan, Sept. 2009.

[7] K. Takeda, H. Tomeba, and F. Adachi, "Joint Tomlinson-Harashima precoding and frequnecy-domain equalization for broadband single-carrier transmission," IEICE Trans. Commun., V0l. 91-B, No. 1, pp. 258-266, Jan. 2008.

[8] D. Wubben, R. Bohnke, V. Kuhn, and K. D. Kammeyer, "MMSE extension of V-BLAST based on sorted QR decomposition," The IEEE 58th Vehicular Technology Conference (VTC-Fall), Florida, USA, Oct. 2003.

[9] S. Sun, Y. Dai, Z. Lei, K. Higuchi, and H. Kawai, "Pseudo-inverse MMSE based QRD-M algorithm for MIMO OFDM," The IEEE 63rd Vehicular Technology Conference (VTC-Spring), Melbourne, Australia, May. 2006.

[10] G. H. Golub and C. F. van Loan, *Matrix Computations*, 3rd ed. Baltimore, MD, Johns Hopkins Univ. Press, 1996.

[11] J. B. Anderson and S. Mohan, "Sequential coding algorithms: A suever and cost analusis," IEEE Trans. on Commun., Vol. 32, pp. 169-176, Feb. 1984.

[12] F. Adachi and K. Takeda, "Bit error rate analysis of DS-CDMA with joint frequency-domain equalization and antenna diversity combining," IEICE Trans. Commun., vol. E87-B, No. 10, pp.2991-3002, Oct. 2004.